

# A Novel Effective Channel Estimation Scheme Applicable to IEEE 802.11p

(Invited Paper)

Zijun Zhao<sup>1,2</sup>, Miaowen Wen<sup>1</sup>, Xiang Cheng<sup>1,2</sup>, Cheng-Xiang Wang<sup>3,4</sup>, and Bingli Jiao<sup>1</sup><sup>1</sup>School of Electronics Engineering & Computer Science, Peking University, Beijing, 100871, China<sup>2</sup>The State Key Laboratory of Integrated Services Networks, Xidian University, Xi'an, 710071, China<sup>3</sup>School of Information Science and Engineering, Shandong University, Jinan, 250100, China<sup>4</sup>Joint Research Institute for Signal and Image Processing, Heriot-Watt University, Edinburgh, EH14 4AS, UK

Email: {zhaozijun, wenmiaowen, xiangcheng, jiaobl}@pku.edu.cn, cheng-xiang.wang@hw.ac.uk

**Abstract**—In vehicle-to-vehicle (V2V) communication, reliable channel estimation is critical in the successful application of equalization and demodulation due to the extremely time-varying characteristic of V2V channels. Therefore, a great deal of channel estimation schemes have been proposed, e.g., by adding postamble, inserting midambles, and turning the phase tracking pilots into channel estimation pilots. However, most of them necessitate a modification of either the packet structure or the basic function of pilots, resulting in an incompatibility with the orthogonal frequency division multiplexing (OFDM) based IEEE 802.11p standard. Motivated by this, in this paper, we present a novel effective channel estimation scheme without the aforementioned modification. In specific, in the proposed scheme, we first utilize the data symbols to construct pilots and then exploit the correlated characteristic between channels within two adjacent symbols to improve the accuracy of the channel estimates. Analysis and simulation results demonstrate that our proposed scheme outperforms all current ones especially in high signal-to-noise ratio (SNR) regime.

## I. INTRODUCTION

Recently, road safety has been greatly concerned since traffic accidents have become one of the leading causes for death all over the world. V2V communication, as an important component of intelligent transportation system, has been proposed to solve this problem. Over the past decade, V2V communications have been widely investigated and various applications for safety have been developed, such as the cooperative forward collision warning, traffic light optimal speed advisory, remote wireless diagnosis [1], etc. More recently, V2V communication has been standardized, i.e., IEEE 802.11p, which is also referred to as dedicated short range communications standard [2].

Channel state information tracking plays an important role for the IEEE 802.11p receiver since it will remarkably influence the performance of subsequent processes, i.e., equalization, demodulation, and decoding. Being aware of that, various approaches for channel estimation have been proposed. Considering that the inherent drawback of the standard preamble structure may degrade the performance of channel estimations, especially for extremely time-variant V2V channels, some approaches supporting reliable channel estimation were developed by modifying the standard packet structure

[3]–[5]. In [3], an iterative channel estimator was proposed based on discrete prolate spheroidal sequences. In this work, an atypical IEEE 802.11p packet preamble structure was used which had a postamble at the end of OFDM packet. In [4] and [5], a well designed midamble sequence was inserted periodically between data symbols to enable continuous channel estimation. Specifically, this midamble-based channel estimation first obtained the initial channel estimates through preamble and then updated those by exploiting the structure of midambles. Although this kind of approaches can achieve reliable performance, the compatibility with other standard IEEE 802.11p receivers is completely lost.

Therefore, to remain the packet structure of IEEE 802.11p unchanged, many other schemes for channel estimation have been proposed. Among them, the most commonly used channel estimation scheme is called least square (LS) estimation, where the channel estimation is performed by employing the predefined two long training symbols ahead of each packet. LS estimation is also a conventional channel estimation scheme for IEEE 802.11a systems and proved to be very effective in relatively stationary indoor environments. However, owing to the extremely time-varying characteristic of V2V channels, those channel estimates derived from training symbols may fail to track the channel response in the DATA field followed behind the training symbols, leading to a serious degradation of the overall system performance. To improve the accuracy of the channel estimation, an approach named as spectral temporal averaging (STA) was proposed in [6]. In this work, the channel response was averaged in the frequency domain and time domain successively to adjust to the dynamic nature of the V2V channels. However, the parameters in this scheme are mostly determined empirically and vary for different types of V2V channels. On the other hand, although STA scheme exhibits superior performance over the LS scheme, it still introduces an unremovable error floor in a high SNR regime.

To fill the aforementioned gap, in this paper, we propose a novel scheme to estimate the V2V channel based on the IEEE 802.11p standard structure. The data symbols are first used to construct pilots and then the correlated characteristic between channels within two adjacent symbols is exploited to improve

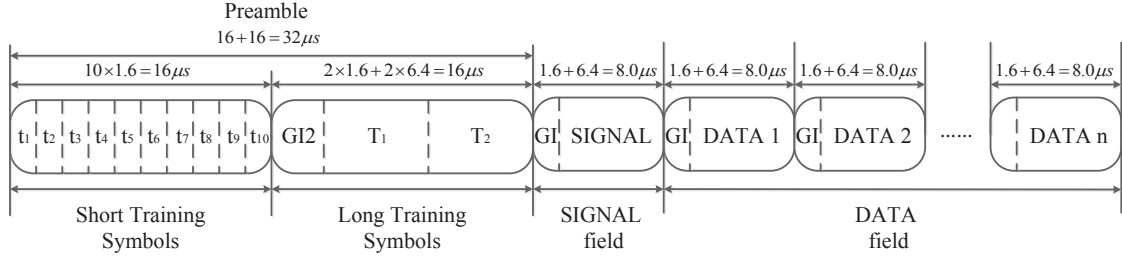


Fig. 1. IEEE 802.11p packet preamble structure.

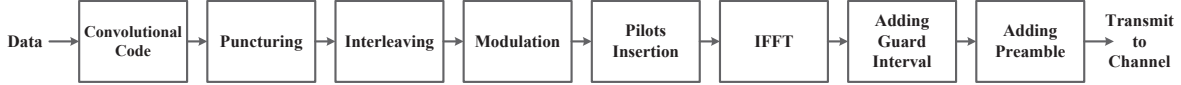


Fig. 2. Block diagram of the IEEE 802.11p transmitter.

the accuracy of the channel estimates. Simulation results demonstrate that our proposed channel estimation scheme outperforms other schemes, especially in a high SNR regime.

The rest of this paper is organized as follows. In Section II, we introduce the structure of IEEE 802.11p and the channel model. Section III gives a brief description of the previous schemes and the proposed scheme for channel estimation. In Section IV, simulation results are presented for performance comparison. Finally, Section V concludes this paper.

## II. SYSTEM MODEL

### A. Structure of IEEE 802.11p

The IEEE 802.11p PHY layer is based on orthogonal frequency division multiplexing (OFDM). Depending on different modulation and puncturing schemes, it can support data transmission rates ranging from 3 to 27Mbps. The packet preamble structure of IEEE 802.11p is shown in Fig. 1. It has almost the same structure as that of IEEE 802.11a except the doubled symbol duration. Each packet consists of preamble including short training symbols and long training symbols, SIGNAL field, and DATA field. The ten  $1.6 \mu s$  short training symbols ( $t_1$  to  $t_{10}$ ) located at the beginning of every packet are used for coarse synchronization. The follow-up two  $6.4 \mu s$  long training symbols  $T_1$  and  $T_2$  are used for fine synchronization and channel estimation. The guard interval (GI) is inserted so as to mitigate inter-symbol interference. The SIGNAL field consists of only one OFDM symbol, while the number of symbols in DATA field are not explicitly defined. Considering that the simulation parameters can be covered in the initial setup, the SIGNAL field is excluded.

Fig. 2 depicts the general block diagram of the IEEE 802.11p transmitter. A convolutional encoder is employed at the beginning for forward error correction. Higher data rate can be gained by using puncturing, e.g.,  $2/3$  and  $3/4$ . The coded data is then interleaved so as to mitigate burst errors caused by pulse noises. Afterward, a modulation such as BPSK, QPSK,

16QAM or 64QAM is implemented. The following 64-point inverse fast fourier transform (IFFT) realizes OFDM modulation. The 64 OFDM subcarriers include 48 data subcarriers and 4 phase tracking pilot subcarriers, located on subcarriers  $-21$ ,  $-7$ ,  $7$ , and  $21$ , are used for compensating the common phase rotation caused by the residual frequency offset. In addition, 11 virtual subcarriers as well as a direct current subcarrier are also added to realize 64-point IFFT. Finally, GI and preamble are inserted.

### B. Channel Model

V2V channel has been investigated in a number of literature (see [8]–[12] and the references therein). In [11] and [12], two different kinds of classical tapped delay line channel models were proposed. The former one is a Wide Sense Stationary Uncorrelated Scattering (WSSUS) model, while the latter one is a non-WSSUS model.

In this paper, we adopt the channel model proposed in [11], which is accepted as the standard V2V channel model in the IEEE 802.11p. The measurement campaign was implemented in the metropolitan Atlanta, Georgia area including six scenarios, i.e., vehicle-to-vehicle (VTV) Expressway Oncoming, VTV Urban Canyon Oncoming, roadside-to-vehicle (RTV) Suburban Street, RTV Expressway, VTV Expressway Same Direction with Wall, and RTV Urban Canyon.

Due to page limit, we cannot give all the simulation results under the six vehicular scenarios shown in [11]. The simulations in this paper are all derived from the first scenario, i.e., VTV Expressway Oncoming. In this scenario, the V2V channel is remarkably deteriorated by the Doppler spread arisen from the oncoming two cars of speed about 104 km/h each on the expressway.

## III. CHANNEL ESTIMATION SCHEMES

As discussed in [7], the placement of pilot symbols in the OFDM time-frequency grid is of crucial importance. When designing a wireless system, the adjacent pilot symbols in

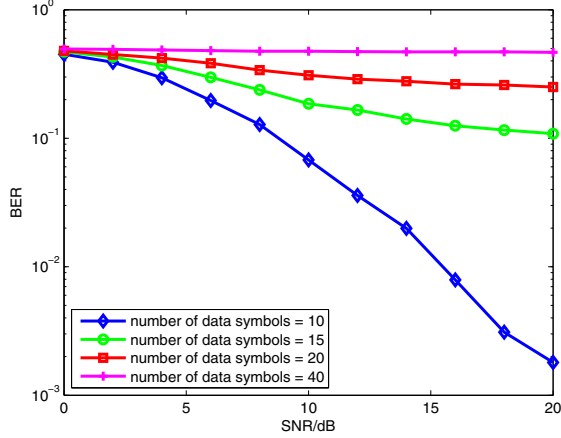


Fig. 3. Comparison of the BER performance with different data symbol lengths using LS estimation.

the time-frequency grid should fulfill some requirements. Specifically, the maximum pilot spacing  $\Delta_f$  in the frequency domain is determined by the maximum excess delay  $\tau_{\max}$

$$\Delta_f \leq \frac{N}{\tau_{\max} B} \quad (1)$$

where  $N$  is the point number of FFT/IFFT, i.e., 64, and  $B$  is the bandwidth of the system. The maximum spacing  $\Delta_t$  in the time domain is limited as

$$\Delta_t = \frac{B}{2f_d(N + G)} \quad (2)$$

where  $G = 16$  represents the length of guard interval.

From the data shown in [11],  $\tau_{\max}$  is  $0.7 \mu s$  and  $f_d$  is approximately about 1.2–1.5 kHz. We can see that the pilot pattern of the IEEE 802.11p satisfies (2) well. However, the 4 phase tracking pilot subcarriers are not spaced closely enough to sample the variation of the channel in the frequency domain, i.e., not fulfilling (1). Therefore, those pilots can be hardly employed for channel estimation only.

#### A. Previous Schemes

1) As mentioned before, a common manner of channel estimation for the IEEE 802.11 is the LS estimation. It jointly makes use of the received preamble  $R_{T_1}(k)$  and  $R_{T_2}(k)$  ahead of data symbols, i.e., the two long training symbols  $T_1$  and  $T_2$  shown in Fig.1, to estimate the channel response

$$H(k) = \frac{R_{T_1}(k) + R_{T_2}(k)}{2X(k)} \quad (3)$$

where  $X(k)$  is the predefined frequency domain long training symbol. The channel response derived from (3) is then used for the subsequent equalization assuming that the channel is stationary for one packet. However, the V2V channel actually changes very fast and thus the LS estimation will significantly deteriorate the system performance in a practical use.

Fig. 3 demonstrates the comparison of the bit error rate (BER) performance with different numbers of data symbols using LS estimation. As expected, with the increase of packet

length, the system performance degrades seriously, especially when the number of data symbols is more than 10, the error floor emerges. A solution to this problem is to decrease the packet length, but, at the same time, it may reduce the system efficiency.

2) To figure out the drawback of LS estimation, a scheme called STA was proposed in [6]. In this work, STA was defined as an enhanced equalization scheme, but actually, it is an approach to estimate the time-variant channel.

In the STA scheme, the  $(i-1)$ th estimated channel response  $H_{STA,i-1}(k)$  is first used to equalize the received data symbol  $S_{R,i}(k)$ , gives

$$\hat{S}_{T,i}(k) = \frac{S_{R,i}(k)}{H_{STA,i-1}(k)} \quad (4)$$

where  $i$  represents the number of the data symbol and  $H_{STA,0}(k)$  is derived from (3) by using the two long training symbols and defined as the 0th data symbol's channel response. Note that, the symbols on the 4 phase tracking pilot subcarriers are not equalized in (4).  $\hat{S}_{T,i}(k)$  is then demapped to obtain  $\hat{X}_i(k)$ . For completeness, those  $\hat{X}_i(k)$  with  $k = -21, -7, 7, 21$ , i.e., the demapped symbols on the phase tracking pilot subcarriers, are endowed with the frequency domain values predefined in the standard. The initial channel estimate,  $H_i(k)$  is estimated as

$$H_i(k) = \frac{S_{R,i}(k)}{\hat{X}_i(k)} \quad (5)$$

It was further considered in [6] that since  $H_i(k)$  was derived directly from the data symbols which may be incorrectly demapped, an averaging of the initial estimates in both frequency and time domain was needed to improve the accuracy. The frequency domain averaging is implemented as

$$H_{update}(k) = \sum_{\lambda=-\beta}^{\lambda=\beta} \omega_\lambda H_i(k + \lambda) \quad (6)$$

where  $2\beta + 1$  represents the number of subcarrier that is averaged and  $\omega_\lambda$  is a set of weighting coefficients with unit sum which are often assumed as an equal value, i.e.,  $\omega_\lambda = 1/(2\beta + 1)$ . The time-domain averaging is completed as follows which also turns out to be the final channel estimate,

$$H_{STA,i}(k) = \left(1 - \frac{1}{\alpha}\right) H_{STA,i-1}(k) + \frac{1}{\alpha} H_{update}(k) \quad (7)$$

where  $\alpha$  is an updating parameter related to the Doppler spread. The parameters  $\alpha$  and  $\beta$  depend on the different types of V2V channels. To ensure accuracy,  $\alpha$  and  $\beta$  should be determined from the knowledge of the radio environment, e.g., from Global Positioning System and map knowledge referred in [6]. However, it is hard to obtain these kind of environment information in practice. Therefore, it was suggested in [6] that for simplicity and convenience, fixed values were chosen with performance degradation at an acceptable level.

#### B. Proposed Scheme

Although the aforementioned schemes are effective in estimating the channel in some cases, they still have several limitations, e.g., limited packet length and impractical application.

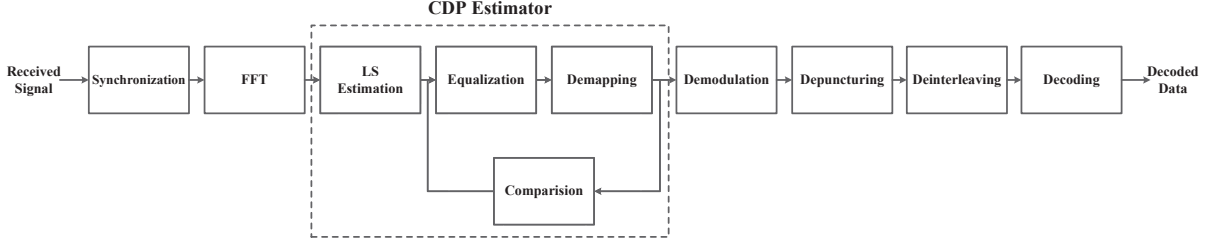


Fig. 4. CDP receiver

In order to improve the performance of the channel estimation in time-variant V2V channels, we introduce a novel estimation scheme by using preamble-based estimated channel response and constructed data pilots (CDP).

Fig. 4 shows the block diagram of the receiver, in which the dashed box demonstrates the CDP estimator, which is implemented between the FFT and demodulation operations.  $S_{R,i}(k)$  is the frequency-domain received symbol on the  $k$ th subcarrier obtained from FFT, i.e., OFDM demodulation. Note that,  $k$  represents the 48 data subcarriers without taking consideration of the 4 pilot subcarriers. CDP estimator iteratively updates the channel estimate under the assumption that the channel response of the adjacent two data symbols have high correlation. Therefore, the first equalization is performed as

$$\hat{S}_{T,i}(k) = \frac{S_{R,i}(k)}{H_{CDP,i-1}(k)} \quad (8)$$

where  $H_{CDP,i-1}(k)$  is the output of the previous estimation process, i.e.,  $(i-1)$ th symbol's estimated channel response.

$\hat{S}_{T,i}(k)$  is then demapped to construct data pilots  $\hat{X}_i(k)$ , the same as that in STA scheme. Owing to the impacts of noise and other interferences,  $\hat{S}_{T,i}(k)$  is possibly located into the wrong regions. Therefore,  $\hat{X}_i(k)$  is easily to be demapped to the incorrect constellation points. However, the error can be mitigated to a certain degree in the following steps by exploiting the correlated characteristic between channels within two adjacent symbols.

The constructed data pilot  $\hat{X}_i(k)$  is then employed to calculate the  $i$ th data symbol's channel response by using (5), i.e., the LS estimation. Note that  $H_i(k)$  is a relatively accurate estimated channel response, however, it is not the final output of the CDP estimator and it will be subsequently used to equalize  $S_{R,i-1}(k)$  such that

$$\hat{S}'_{C,i-1}(k) = \frac{S_{R,i-1}(k)}{H_i(k)}. \quad (9)$$

$S_{R,i-1}(k)$  is also equalized by  $H_{CDP,i-1}(k)$  which we have used in (8). The equalized  $\hat{S}''_{C,i-1}(k)$  is given by

$$\hat{S}''_{C,i-1}(k) = \frac{S_{R,i-1}(k)}{H_{CDP,i-1}(k)}. \quad (10)$$

To compare  $\hat{S}'_{C,i-1}(k)$  and  $\hat{S}''_{C,i-1}(k)$ , they should be demapped to the constellation points  $\hat{X}'_{i-1}(k)$  and  $\hat{X}''_{i-1}(k)$  first according to the modulation scheme. Since we have assumed before that the two adjacent data symbols have high

correlation, if  $\hat{X}'_{i-1}(k) \neq \hat{X}''_{i-1}(k)$ , it indicates that the  $k$ th subcarrier's  $\hat{X}_i(k)$ , which demapped after (8) is incorrect and we should define that  $H_{CDP,i}(k) = H_{CDP,i-1}(k)$ , i.e., the previous symbol's estimated channel response. Otherwise, if  $\hat{X}'_{i-1}(k) = \hat{X}''_{i-1}(k)$ , we have  $H_{CDP,i}(k) = H_i(k)$ .

It is noticeable that the condition for the previous channel estimation steps is  $i > 1$  and  $i = 1$  is excluded. The reason is that the two long training symbols are BPSK modulated to 1 and -1. However, data symbols are possibly modulated by other schemes instead of BPSK. Hence, (9) cannot be employed owing to the different modulation schemes. In addition, to ensure accuracy, the channel response derived from (3) cannot be defined as  $H_{CDP,1}(k)$  directly. Therefore, (9) should be modified to

$$\hat{S}'_{C,0}(k) = \text{real} \left( \frac{R_{T_2}(k)}{H_1(k)} \right) \quad (11)$$

where  $R_{T_2}(k)$  is the second long training symbol received after FFT. If  $\hat{S}'_{C,0}(k) > 0$ , we have  $\hat{X}'_0(k) = 1$ , or else  $\hat{X}'_0(k) = -1$ . Note that,  $\hat{X}'_0(k)$  is the known frequency-domain transmitted signal. Afterwards,  $\hat{X}'_0(k)$  and  $\hat{X}''_0(k)$  are compared with finally derive  $H_{CDP,1}(k)$ . If  $\hat{X}'_0(k) = \hat{X}''_0(k)$ , we have  $H_{CDP,1}(k) = H_1(k)$ ; otherwise, we have  $H_{CDP,1}(k) = H(k)$ , where  $H(k)$  is obtained from (3).

#### IV. SIMULATION RESULTS AND ANALYSIS

In this section, BER simulations are conducted. In the simulations, the LS and STA schemes are taken as two representative examples for performance comparison with our proposed scheme. To achieve the optimal performance of the STA scheme, we set parameters  $\alpha = \beta = 2$  as in [6].

Figs. 5 and 6 show the comparison of the LS, STA, and CDP schemes in BER performance of BPSK and 16QAM, respectively. To evaluate the performance of the IEEE 802.11p with different packet lengths, the numbers of OFDM symbols are chosen to be 40 and 80. The figures depict that smaller packet length is beneficial for the BER performance, especially for STA and CDP schemes. As expected, the LS scheme keeps on a relatively high level of BER for both QPSK and 16QAM, while much smaller BERs are achieved by the STA and CDP schemes. In a very low SNR regime where the BER is around 0.5, STA scheme outperforms CDP scheme. When the SNR is high enough, CDP scheme offers a significant improvement over the STA scheme. This is because that when the SNR is

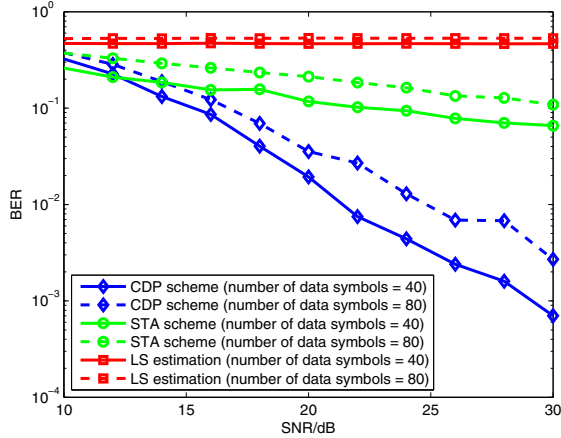


Fig. 5. Comparison of the BER performance of the LS, STA, and CDP schemes in QPSK modulation.

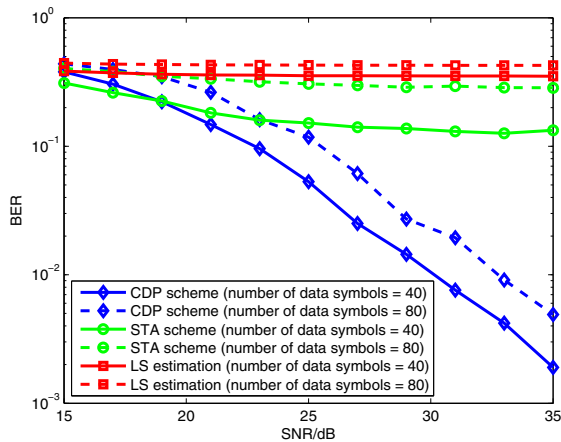


Fig. 6. Comparison of the BER performance of the LS, STA, and CDP schemes in 16QAM modulation.

low, the noise and interference are powerful enough to shift  $\hat{S}_{T,i}(k)$  to wrong regions and as a result,  $\hat{X}_i(k)$  are demapped to incorrect constellation points. As the SNR increases, the aforementioned influence is reduced and thus the superiority of the CDP scheme emerges. We remark that the impact from error demapping has been mitigated to a certain degree by the exploitation of the correlated characteristic of V2V channels. However, due to the extremely time-varying characteristic caused by high Doppler shift in the adopted V2V Expressway Oncoming channel scenario, such improvement seems not to be significant for a medium SNR regime. For the other five channel scenarios where the Doppler shift is much smaller as mentioned in Section II, the overwhelming performance of the CDP scheme over the STA scheme will be foreseen.

## V. CONCLUSIONS

In this paper, we have focused on the channel estimation problem encountered in V2V communications. The issue is

raised due to the inherent dynamic nature of V2V channels. To solve this problem, we have proposed a channel estimation scheme by constructing pilots using the data symbols and properly exploiting the correlated characteristic of V2V channels. Unlike most previous work, the proposed scheme adheres to the structure of the standard and is independent on what type of V2V channels. Therefore, the proposed scheme is not only compatible with other IEEE 802.11p receivers but also applicable to different V2V scenarios. Simulation results have shown that the BER performance of our proposed scheme outperforms all the current ones, especially in a high SNR regime.

## VI. ACKNOWLEDGMENT

This work was jointly supported by the National Natural Science Foundation of China (Grant no. 61101079& 61210002), the Science Foundation for the Youth Scholar of Ministry of Education of China (Grant no. 20110001120129), the State Key Laboratory of Integrated Services Networks, Xidian University (Grant no. ISN13-05), and the RCUK for the UK-China Science Bridges Project: R&D on (B)4G Wireless Mobile Communications.

## REFERENCES

- [1] H. Hartenstein and K. P. Laberteaux, "A Tutorial Survey on Vehicular Ad Hoc Networks," *IEEE Commun. Mag.*, vol. 46, no. 6, pp. 164–171, Jun. 2008.
- [2] *802.11p-2010 IEEE Standard for Information Technology—Telecommunications and Information Exchange Between Systems—Local and Metropolitan Area Networks—Specific Requirements Part 11, Wireless LAN Medium Access Control (MAC) and Physical Layer (PHY) Spec.*, 2010.
- [3] T. Zemen, L. Bernad, N. Czink, and A. F. Molisch, "Iterative Time-Variant Channel Estimation for 802.11p Using Generalized Discrete Prolate Spheroidal Sequences," *IEEE Trans. on Veh. Tech.*, vol. 61, no. 3, pp. 1222–1233, Mar. 2012.
- [4] S. I. Kim, H. S. Oh, and H. K. Choi, "Mid-amble Aided OFDM Performance Analysis in High Mobility Vehicular Channel," *Proc. of Intelligent Vehicles Symposium*, pp. 751–754, Jun. 2008.
- [5] W. Cho, S. I. Kim, H. K. Choi, H. S. Oh, and D. Y. Kwak, "Performance Evaluation of V2V/V2I Communications: The Effect of Midamble Insertion," *Proc. Wireless VITAE'09*, pp. 793–797, May. 2009.
- [6] J. A. Fernandez, K. Borries, L. Cheng, B. V. K. Vijaya Kumar, D. D. Stancil, and F. Bai, "Performance of the 802.11p Physical Layer in Vehicle-to-Vehicle Environments," *IEEE Trans. on Veh. Tech.*, vol. 61, no. 1, pp. 3–14, Jan. 2012.
- [7] C. F. Mecklenbräuker, A. F. Molisch, J. Karedal, F. Tufvesson, A. Paier, L. Bernad, T. Zemen, O. Klemp, and N. Czink, "Vehicular Channel Characterization and its Implications for Wireless System Design and Performance," *Proc. IEEE*, vol. 99, no. 7, pp. 1189–1212, Jul. 2011.
- [8] C. Wang, X. Cheng, and D. I. Laurenson, "Vehicle-to-Vehicle Channel Modeling and Measurements: Recent Advances and Future Challenges," *IEEE Commun. Mag.*, vol. 47, no. 11, pp. 96–103, Nov. 2009.
- [9] X. Cheng, C. Wang, D. I. Laurenson, S. Salous, and A. V. Vasilakos, "An Adaptive Geometry-Based Stochastic Model for Non-Isotropic MIMO Mobile-to-Mobile channels," *IEEE Trans. Wireless Comm.*, vol. 8, no. 9, pp. 4824–4835, Sept. 2009.
- [10] X. Cheng, C. Wang, H. Wang, X. Gao, X. You, D. Yuan, B. Ai, Q. Huo, L. Song, and B. Jiao, "Cooperative MIMO channel modeling and multi-link spatial correlation properties," *IEEE Journal on Selected Areas in Communications*, vol. 30, no. 2, pp. 388–396, Feb. 2012.
- [11] G. Acosta-Marum and M. A. Ingram, "Six Time-and Frequency-Selective Empirical Channel Models for Vehicular Wireless LANs," *IEEE Veh. Tech. Mag.*, vol. 2, no. 4, pp. 4–11, Dec. 2007.
- [12] I. Sen and D. W. Matolak, "Vehicle-Vehicle Channel Models for the 5-GHz Band," *IEEE Trans. Intelligent Transportation Systems*, vol. 9, no. 2, pp. 235–245, Jun. 2008.